

MEMO

Authors: J.E Campagne. A.S. Torrentó
Nançay/Amas/12.12.11

Diffusion : R. Ansari, P. Colom, Ch. Magneville, J. M. Martin, M. Moniez

Objet: Data calibration for Abell85, Abell1205 and Abell2440 (2011) using DAB signals.

1 Introduction

The DAB (“diode à bruit”) is used for the Nançay Radio Telescope (NRT) calibration, i.e. converting the arbitrary units measured by the electronics into Jansky. In this note we investigate the utilization of the DAB to calibrate the BAO data. Firstly we explain the calculation of the calibration coefficients and show the values obtained for Abell 85, Abell 1205 and Abell 2440 clusters. Then, we study the effect of the calibration in the signals. We finally show the frequency dependence of the DAB signal and compare it two other data sets: the analysis of PKS1127-14 with a ROACH board by P. Colom et al., and preliminary analysis of few data taken with BAO electronics on NGC4383 (ON-OFF).

2 Calculation of calibration coefficients

The calibration of the DAB is done through the measurement of a source with known flux. Let us suppose that the RT follows regularly a calibration source and compares it to the signal delivered by a stable noise device (noted DAB hereafter). Then, at a given frequency (not shown but it is implicit) one has the following very simple relationships between signal from the source and from the DAB:

$$\begin{aligned} I(Jy)_S^{RT} &= C^{RT} * I(a.u)_S^{RT} \\ I(Jy)_{DAB}^{RT} &= C^{RT} * I(a.u)_{DAB}^{RT} \end{aligned}$$

So, thanks to the source one can express the RT DAB signal in Jy as:

$$I(Jy)_{DAB}^{RT} = \frac{I(Jy)_S^{RT}}{I(a.u)_S^{RT}} * I(a.u)_{DAB}^{RT}$$

Similarly, in principle the same relation occurs for the BAO electronic chain as

$$I(Jy)_{DAB}^{BAO} = \frac{I(Jy)_S^{BAO}}{I(a.u)_S^{BAO}} * I(a.u)_{DAB}^{BAO}$$

But, the BAO chain has not yet the opportunity to take data of a calibration source. So, firstly we take for granted that the intensity of the DAB is the same as measured by the

RT and the BAO chains, so $I(Jy)_{DAB}^{BAO} = I(Jy)_{DAB}^{RT} = I(Jy)_{DAB}$, and secondly for another source S' (or signal) observed at the same frequency, we get using the above formula:

$$I(Jy)_{S'}^{BAO} = \frac{I(a.u.)_{S'}^{BAO}}{I(a.u.)_{DAB}^{BAO}} * I(Jy)_{DAB} \quad (1)$$

This is the basic calibration formula only valid at a specific frequency, but the value of $I(Jy)_{DAB}$ is has not been determined with precision yet.

To determine the $I(a.u.)_{DAB}^{BAO}$ coefficient for the BAO electronic chain we proceed as follows (extracted from Nançay/Abell85/21.11.11 MEMO):

- First, for each power spectrum registered every 120ms during 14sec around ON or OFF DAB signals, we compute the power at a given calibration frequency in a 6.25MHz band width. So, we can follow the power time evolution as illustrated in Figure 1. The DAB signal is injected at two distinct positions inside the horn, so in practice it produces generally a 2-levels intensity pattern.

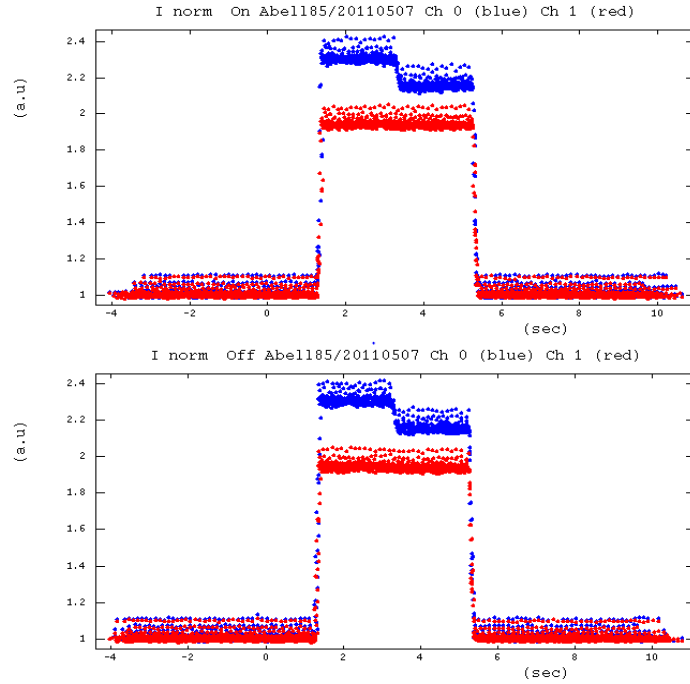


Figure 1 Example of normalized power time evolution cumulated over all cycles of a run (ex. Abell85 May 7th 2011 at 1380MHz in a 6.25MHz band). The $t_0=0$ sec corresponds to the start of the DAB in the SCA file (see Nançay/Abell85/21.11.11).

- Secondly, thanks to the normalization by the gain, one extracts the spectra of the time window $[-3\text{sec}, -1\text{sec}]$ and $[6\text{sec}, 8\text{sec}]$. The mean of these spectra is most probably related to the T_{sys} . Then, by setting a threshold at 20% of the min-max above the min power, the 2-levels pattern is identified and the mean of the two median power of each level is computed. Finally, the difference between this mean power and the T_{sys} is nothing but the BAO coefficient $I(a.u.)_{DAB}^{BAO}$ for each channel, valid for the given cycle of the run (and kept in mind at the given

frequency). The mean value on all the cycles of a run is used on purpose as the unique coefficient valid for that run.

3 Calibration coefficients

For simplicity, all the plots of the note will be taken only from Abell 1205 analysis. The plots obtained for the other clusters (Abell 2440 and Abell 85) lead to the same conclusions and are displayed in the appendices.

In Figure 2, we show the calibration coefficients obtained as explained above as a function of the cycle number in the case of the Abell 1205 cluster. The black dots are the calibration coefficients per cycle and in red we represent the coefficients per run, i.e. the mean of all the cycle coefficients in each run; on top of the figure we see the OFF mode for channels Ch0 (left) and Ch1 (right); similarly we see at the bottom the ON mode also for Ch 0 and Ch1.

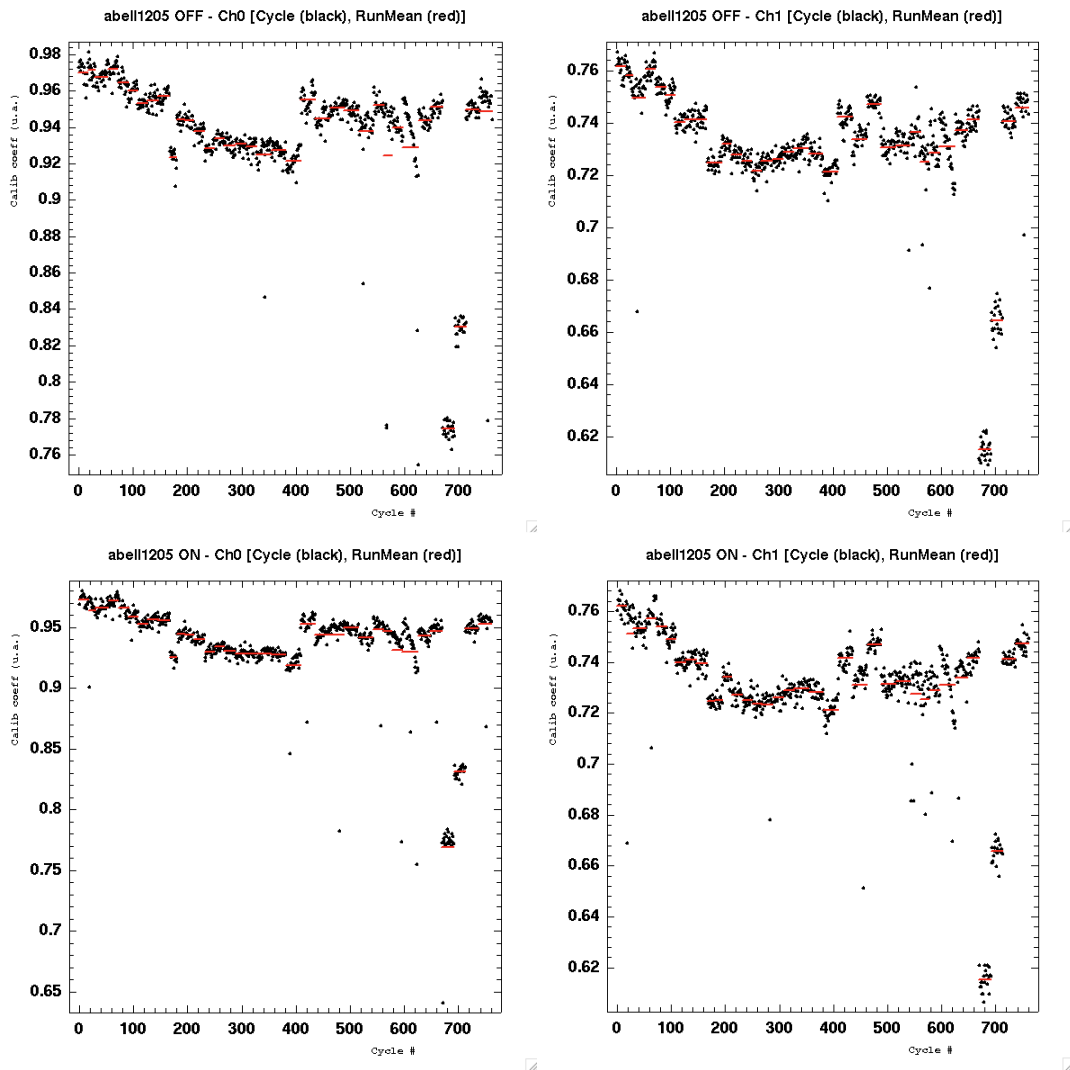


Figure 2. Calibration coefficients per cycle (black) and per run (red) vs. cycle number. Top: ON mode for channels Ch0 (left) and Ch1 (right). Bottom: idem for mode ON.

We observe that within each run the coefficients change in a random way in most of cases. In the whole period the variations are within $\pm 2.5\%$ but with the same systematic

tendency for both channels and ON/OFF modes. Sometimes, a value quite different from the bulk of coefficients is obtained, which affects the determination of the coefficient per run.

The time variation is independent of the overall system noise (T_{sys}), as we show in Figure 3, where we plot the T_{sys} for channel 0 vs. cycle number¹, together with the calibration

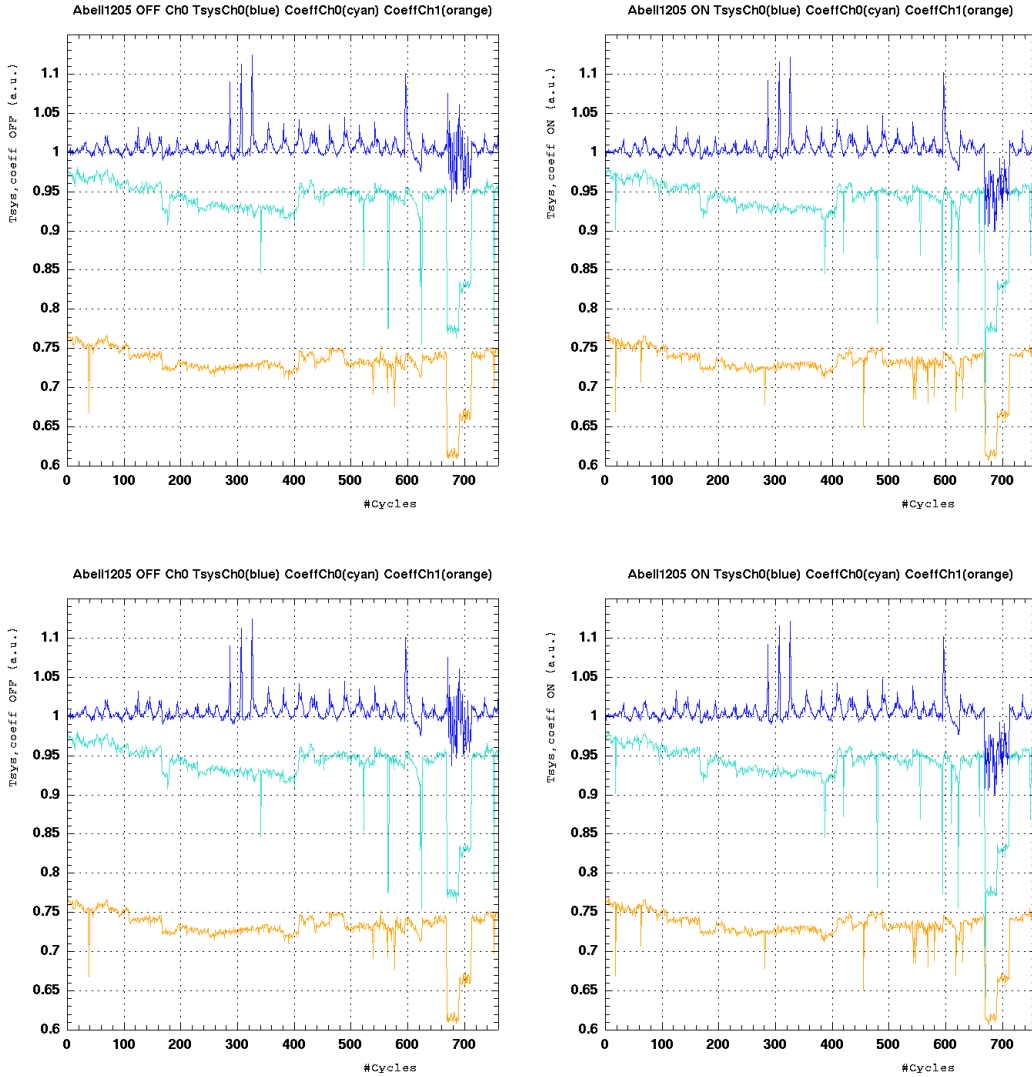


Figure 3. System noise (T_{sys} , blue) and calibration coefficients at 1410MHz for Ch0 (cyan) and Ch1 (orange) vs. cycle number for OFF (left) and ON (right) modes.

coefficients per cycle for Ch0 (cyan) and Ch1 (orange). The T_{sys} is varying from cycle to cycle in a run as expected, but it is noticeable that the minimum value is quite stable along the whole data set (except in September 2011). It is clear from this plot that the BAO calibration coefficients variations are intrinsic to the DAB and are not related to temporal variations of the electronics, which should also have affect the T_{sys} evolution. Thus, applying the calibration correction with the DAB introduce the intrinsic DAB variations in the data, as shown in the following section and already reported in

¹ The T_{sys} for channels 0 and 1 are consistent at $\sim 5 \times 10^{-3}$ level.

Nançay/Abell85/23.11.11, Nançay/Abell1205/23.11.11 and Nançay/Abell2440/23.11.11 MEMOs.

4 Effect of calibration in signal data

To calibrate the data one uses the formula (1), taking $I(a.u.)_S^{BAO}$ as the ON or OFF signals for a given cluster S' (each of them normalized by the gain) and, $I(a.u.)_{DAB\ ON,OFF}^{BAO}$ the corresponding calibration coefficients per run and per cycle determined at $(1410 \pm 3.125)\text{MHz}^2$.

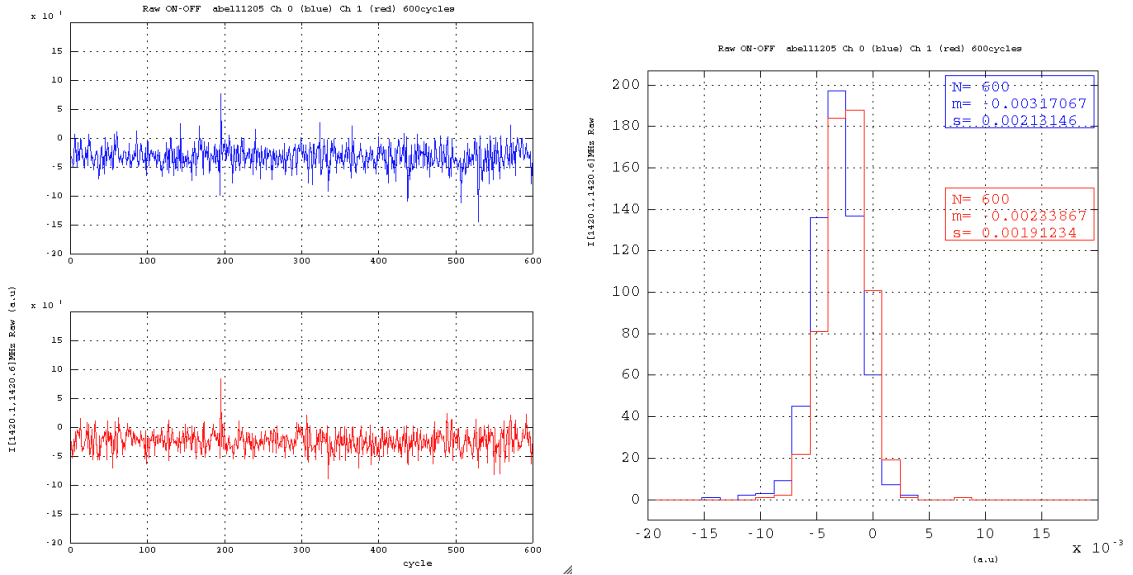


Figure 4. Integrated ON-OFF mean intensity from the galactic HI line without calibration (Abell1205). Signal evolution (left) and mean and sigma of the previous plot (right).

To show the effect of the calibration we take, for example, the difference $ON/I(a.u.)_{DAB\ ON}^{BAO} - OFF/I(a.u.)_{DAB\ OFF}^{BAO}$ integrated in the typical range $[1420.1, 1420.4]\text{MHz}$ and we plot it as a function of the cycle number without calibration³ (Figure 4), with calibration per run (Figure 5) and with calibration per cycle (Figure 6), together with the corresponding mean and standard deviation. Notice the change of vertical scale in the latter figure.

² The calibration coefficients are not supposed to vary very much between 1410MHz and 1420MHz.

³ $I(a.u.)_{DAB\ ON}^{BAO} = I(a.u.)_{DAB\ OFF}^{BAO} = 1$ for this case.

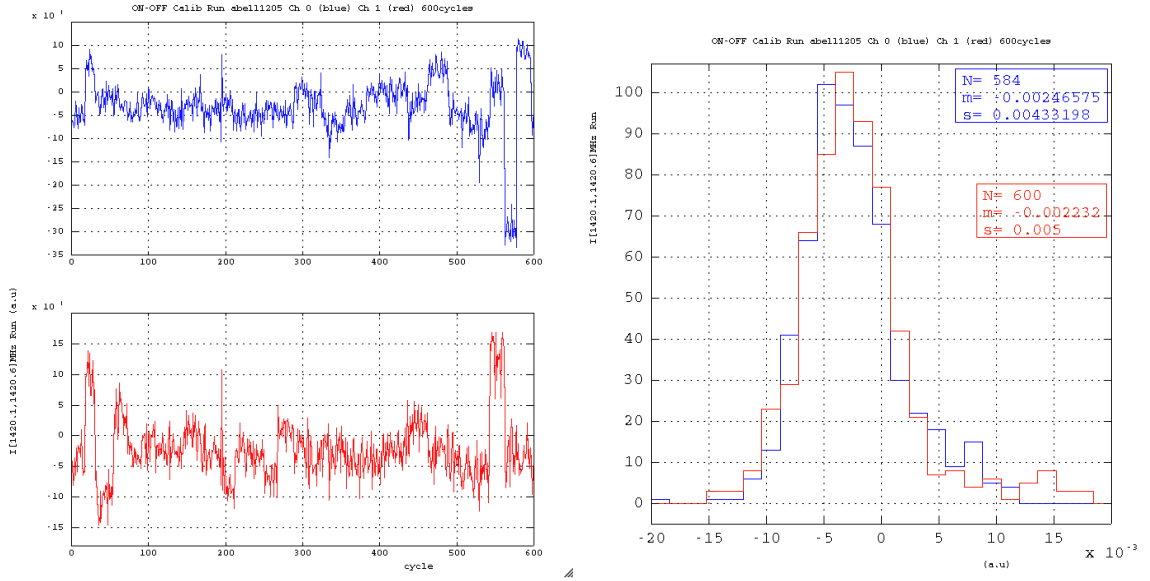


Figure 5. Integrated ON-OFF intensity from the galactic HI line calibrated with coefficients “per run” (Abell1205). Signal evolution (left) and mean and sigma of the previous plot (right).

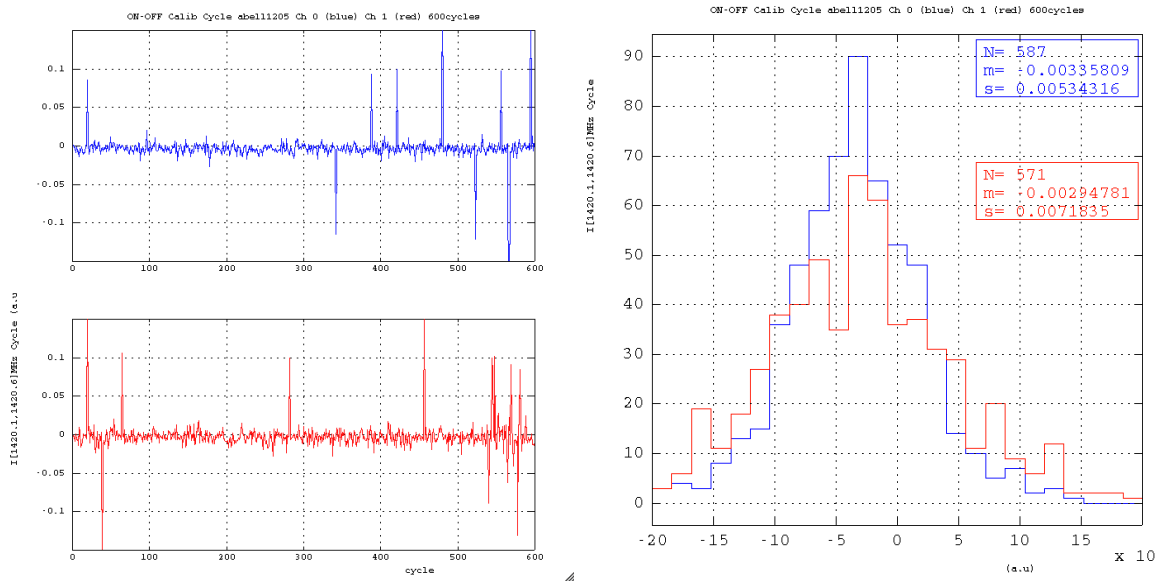


Figure 6. Integrated ON-OFF intensity from the galactic HI line calibrated with coefficients “per cycle” (Abell1205). Signal evolution (left) and mean and sigma of the previous plot (right).

We clearly see that the non-calibrated plot is much more stable than the calibrated ones. The variations of T_{sys} are well absorbed by the ON-OFF operation, leaving a dispersion of $\sim 2 \times 10^{-3}$ a.u.

The differences between the calibration coefficients per run translate into a signal evolution showing the run pattern. The standard deviation of the resulting signal is wider than above, i.e. $\sigma \sim 4 \times 10^{-3}$ a.u.

The calibration per cycle does not introduce any pattern, but it severely widens the signal up to $\sigma \sim 6 \times 10^{-3}$ a.u., i.e. a 3 times greater than the non-calibrated signal. We also find

signal peaks which correspond to those calibration coefficients falling far from the bulk values of the run.

Thus, we conclude that the stability of the DAB should be investigated if we want to use it to make the calibration of the BAO data. Until this is done, we stick to non-calibrated data to make the cluster analysis. An alternative is to use a calibration galaxy and analyze it directly by BAO electronics.

5 DAB chromaticity and normalization

Up to now, we have shown results using a single calibration frequency. The point is that there exist RT calibrated frequencies: ex. 1280, 1380, 1410MHz. But it is known that the DAB is chromatic, independently of the electronic chain used to acquire the data.

In Figure 7, we represent with green stars the DAB spectrum obtained during the observation of the PKS1127-14 radio source in June 2011 for the “Voie E” in the frequency band [1100, 1580] MHz, using WIBAR (ROACH card) electronics (ref. M. Musa, Rapport de stage DUT mesures physiques option MCPC 2e année (2010-11), « *Etalonnage du grand radiotélescope de Nançay en bande large* »). The resulting spectrum has been normalized by the system-passing band.

We superimpose in the same plot the DAB spectrum obtained using the BAO electronics

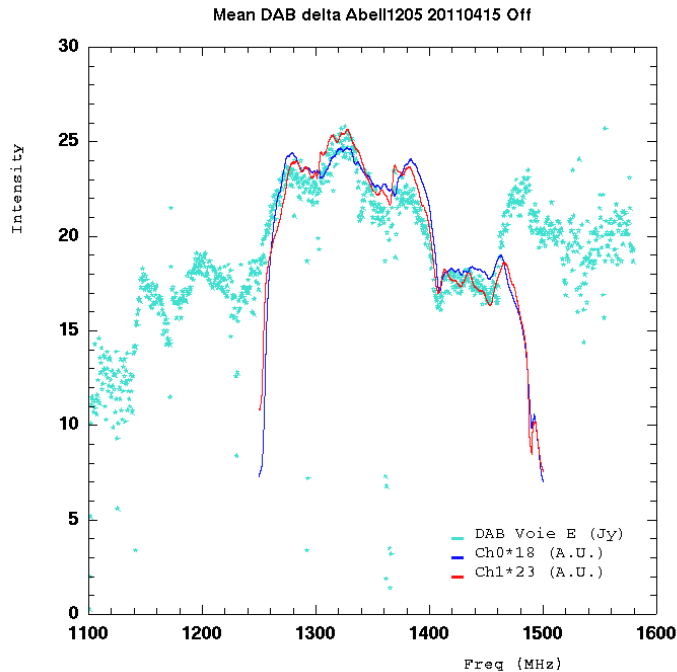


Figure 7. DAB calibrated spectrum (Jy) obtained for the «Voie E» with the WIBAR acquisition chain (green stars), and obtained with the BAO electronics for Ch0 (blue) and Ch1 (red). To compare the BAO curves to the calibrated spectrum we have arbitrarily multiplied them by a factor 18 and 23, respectively.

for both channels Ch0 (blue) and Ch1 (red). The curve for each channel is the mean of the two DAB incidences in the horn. To compare the three spectra we guide the eye by arbitrarily multiplying BAO Ch0 by a factor 18 and BAO Ch1 by a factor 23.

The resemblance of the three spectra is quite remarkable, given that in the first case the analogical signals are transmitted through cables to the ADC, whereas the BAO electronics make the digitization in the chariot. We confirm the extreme chromaticity of the DAB in the BAO large band [1250, 1500]MHz which is not to be attributed to cables. In passing, we could say that the “Voie E” is “more equivalent” to BAO channel Ch1 but the difference between Ch0 and Ch1 is tiny.

If we take for granted the DAB power given in Jy from the PKS1127-14 analysis, we could construct a calibration curve by means of dividing the PKS1127-4 power by the BAO power, as shown in Figure 8.

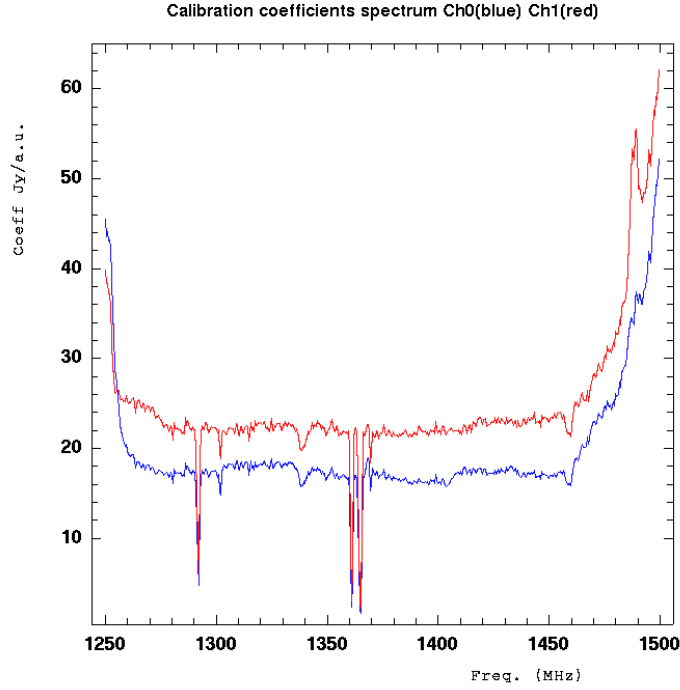


Figure 8. Calibration coefficients in Jy/a.u. as a function of frequency.

Considering the frequency band around 1410MHz, we can argue that the value in a frequency bin of $\Delta\nu$ (30kHz) is given by⁴:

$$\frac{Ch_i}{G_i} (a.u.) \times \Delta\nu \times 2 \times C_{1410}^{DAB} \approx (17 \div 18) \frac{Ch_i}{OFF_i} (Jy) \times \Delta\nu \quad (2)$$

with C_{1410}^{DAB} the coefficient to transform 1 BAO polarization into the total power at 1410MHz of the DAB, and (17÷18) Jy the power at that frequency taken from Figure 7.

Thus, the conversion coefficient value is about (see Figure 8)

$$C_{1410}^{DAB} \approx \frac{(17.0 \div 22.3) \pm 0.5}{2} \approx (8.5 \div 11.6) \pm 0.3 (Jy/a.u.) \quad (3)$$

⁴ Notice that the OFF_i is in fact the filtered version of the OFF which is close to the G_i value.

where the calibration coefficients 17.0 ± 0.6 Jy/a.u. (Ch0) and 22.3 ± 0.5 Jy/a.u. (Ch1) are the mean \pm sigma of the coefficients shown in Figure 8 in the frequency band [1400, 1420]MHz.

It is in fact interesting to compare with preliminary NGC4383 data. The response of both BAO channels after 4 cycles ON-OFF treated by the standard analysis pipeline is given in Figure 9.

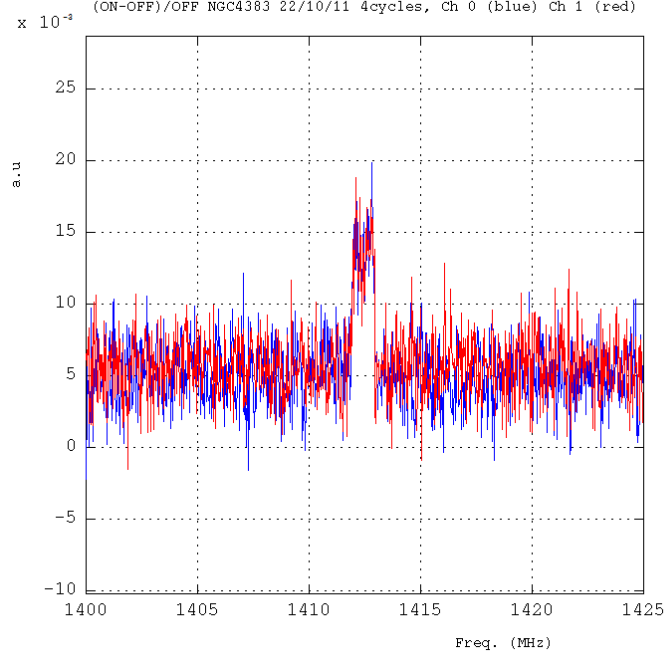


Figure 9 Signal captured after 4 cycles ON-OFF on NGC4383. The HI line reported by A. Chung et al. *Astro. J.* 138:1741–1816, 2009 December has the following characteristics: width of about 213km/s \sim 1MHz and an intensity of 48.4 ± 5.1 Jy.km/s \sim 227mJy.MHz.

The total intensity of the HI line is (227 ± 23) mJy·MHz = (227 ± 23) Jy·kHz above the continuum roughly uniformly distributed among 33 bins of 30kHz (8×10^{-3} a.u. per bin per polarization). So, one can write an equation similar to Eq. 2 as

$$2 \times 33 \times 8 \times 10^{-3} (a.u.) \times 30 (kHz) \times C_{1410}^{NGC} \approx 227 (Jy \cdot kHz)$$

which leads to a conversion coefficient value a bit higher to Eq. 3, as

$$C_{1410}^{NGC} \approx (14.3 \pm 1.4) (Jy / au) \quad (4)$$

This value is about 50% higher than the corresponding coefficient from the DAB.

6 Summary

In this note we have explained how calibration is done in the NRT and how we have obtained calibration coefficients to correct eventually the BAO data through the use of DAB signals taken during the cluster data themselves.

We show that the calibration coefficients “per cycle” vary within a run in (most of times) a random way. In some cases, the coefficient value is very different from the bulk of coefficients for that run. Taking the mean of all the cycle coefficients we obtain calibration coefficients per run that vary slowly from run to run. Considering the whole data set, the variations are within $\pm 2.5\%$ although there is a systematic time evolution.

We have checked that the evolution of the calibration coefficients is independent of the overall system noise (T_{sys}), thus concluding that the variations of the calibration coefficients are due to intrinsic variations of the DAB itself and not to changes in the electronic chain.

We have taken the ON-OFF signal integrated in the HI galactic line for Abell 1205 cluster and applied the calibration “per run” and “per cycle”. The standard deviation of the signal evolution gives an idea of the stability of the DAQ. We see that the calibration “per run” worsens the stability in a factor ~ 2 , and the one “per cycle” in a factor ~ 3 with respect to non-calibrated data. We conclude that the stability of the DAB should be investigated if we want to use it to calibrate the BAO data. In the meantime, we make the analysis of the galaxy clusters with non-calibrated data. In this analysis we have shown that the BAO electronic chain is very stable (except problems in September 2011).

Finally we have studied the frequency dependence of the DAB. We have found the same DAB spectrum from a calibration obtained with the standard NRT electronic chain, where the signals are transferred by cables to the ADC, and from the BAO data where the digitization of the signals is performed directly in the chariot. Taking the opportunity of the DAB calibration by the PKS1127-14 source with the ROACH board by M. Musa, we have obtained a conversion coefficient for a single BAO channel at 1410MHz which turns to be in agreement with preliminary NGC4383 HI line analysis using BAO pipeline with 50% error. The conversion coefficient is about $C_{1410} \approx (9 \div 14)(\text{Jy} / \text{au})$.

A Appendix: Abell 85

We include in this appendix the same plots for the cluster Abell 85 as shown in the note for Abell 1205.

A.1 Calibration coefficients

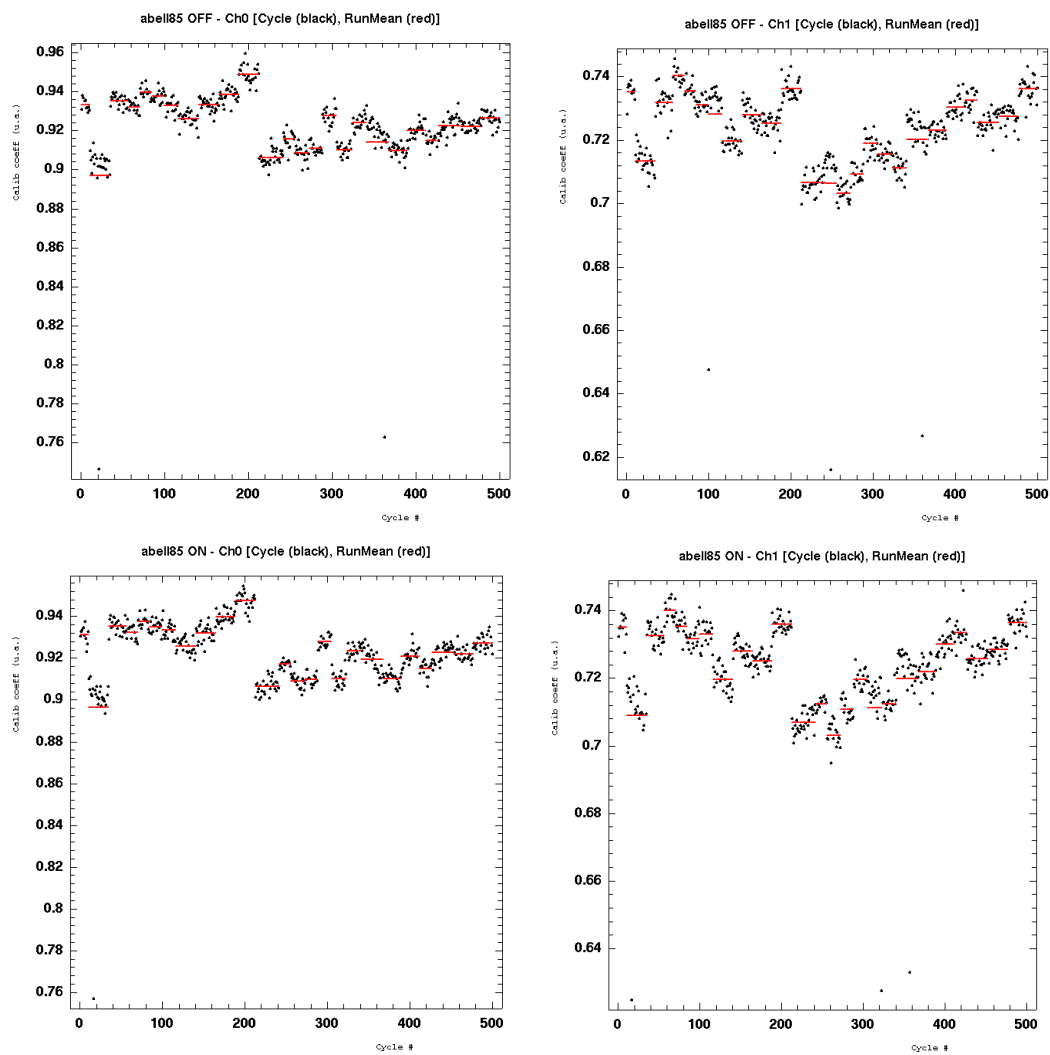


Figure 10. Calibration coefficients per cycle (black) and per run (red) vs. cycle number. Top : ON mode for channel 0 (left) and channel 1 (right). Bottom : idem for mode ON.

A.2 T_{sys} evolution vs. calibration coefficients

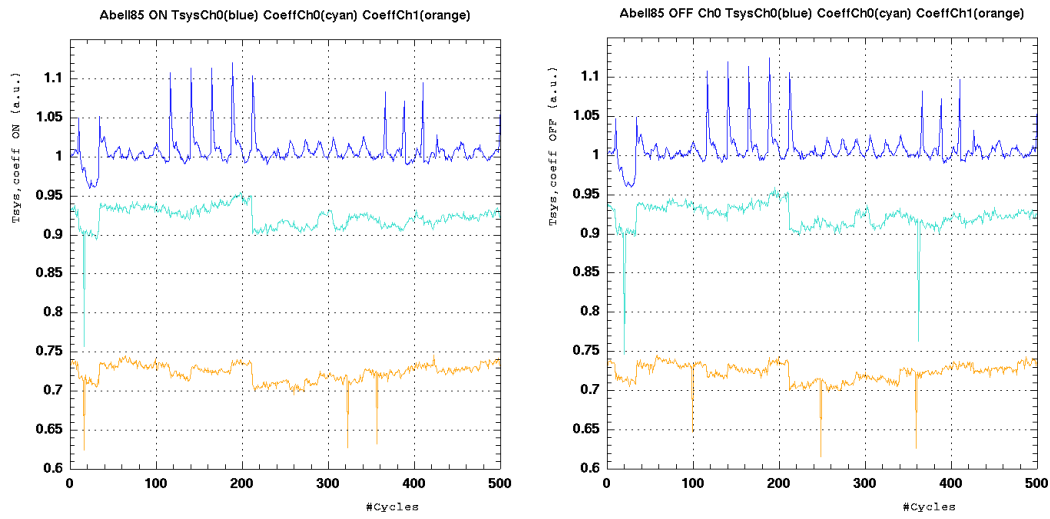


Figure 11. System noise (T_{sys} , blue) and calibration coefficients for Ch0 (cyan) and Ch1 (orange) vs. cycle number for OFF (left) and ON (right) modes.

A.3 Effect of calibration in signal data

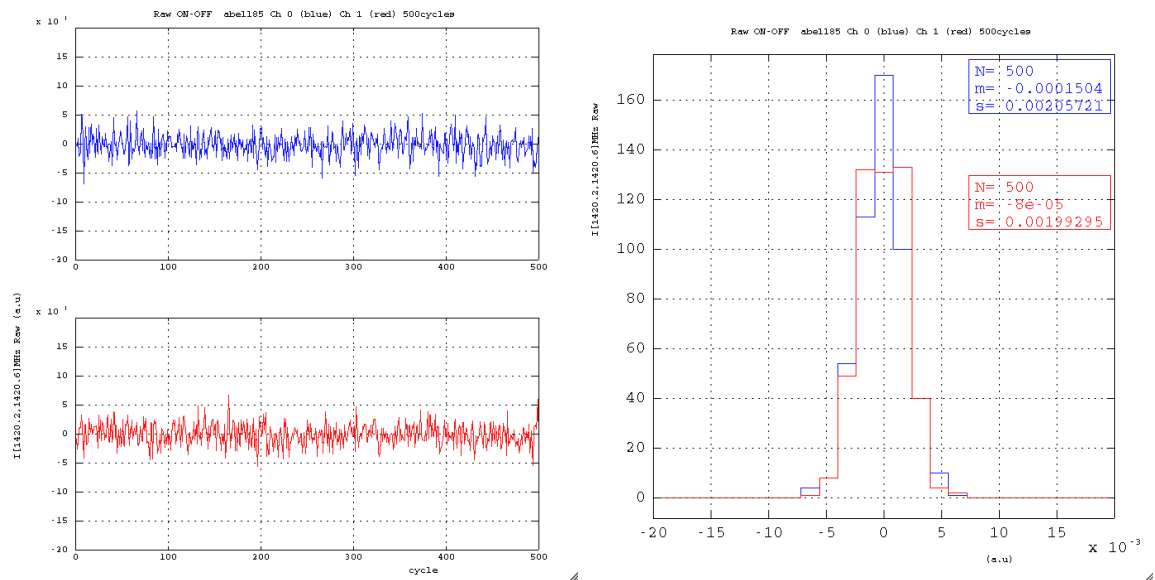


Figure 12. Integrated ON-OFF mean intensity from the galactic HI line without calibration. Signal evolution (left) and mean and sigma of the previous plot (right).

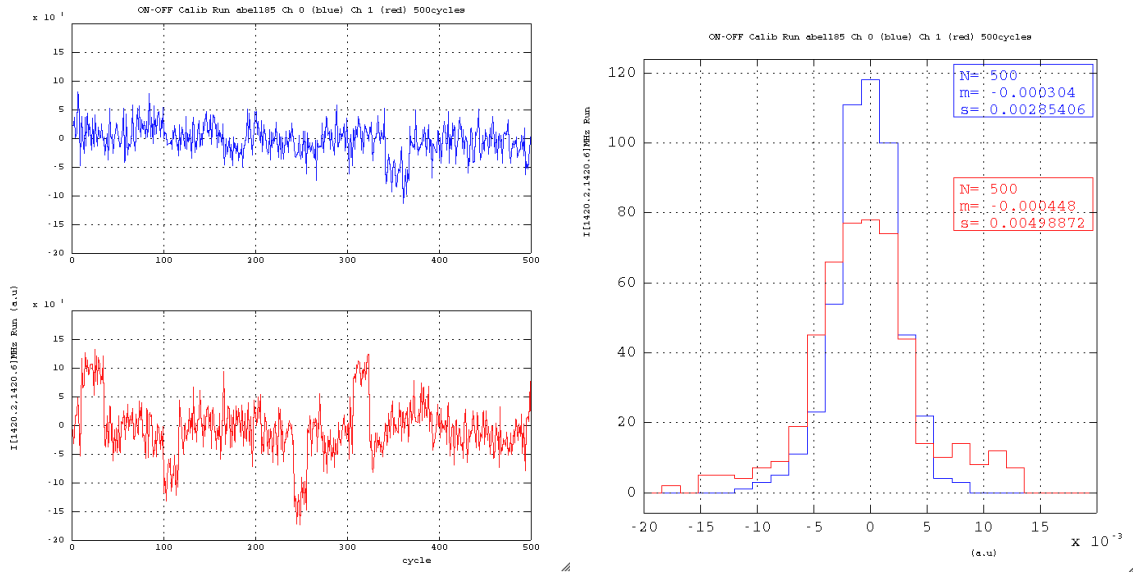


Figure 13. Integrated ON-OFF intensity from the galactic HI line calibrated with coefficients “per run”. Signal evolution (left) and mean and sigma of the previous plot (right).

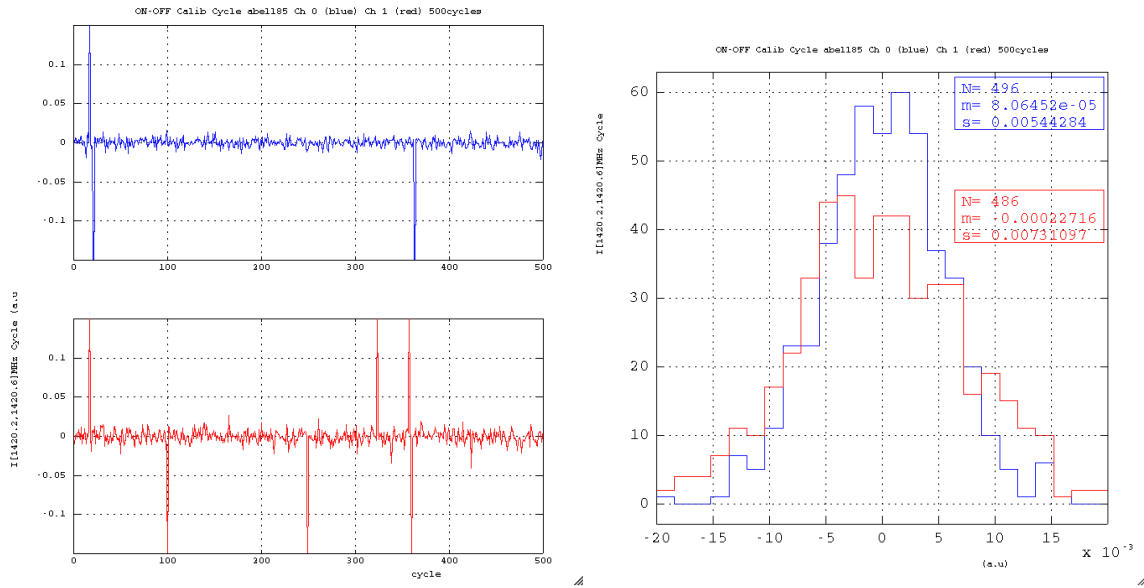


Figure 14. Integrated ON-OFF intensity from the galactic HI line calibrated with coefficients “per cycle”. Signal evolution (left) and mean and sigma of the previous plot (right).

B Appendix: Abell 2440

We include in this appendix the same plots for the cluster Abell 2440 as shown in the note for Abell 1205.

B.1 Calibration coefficients

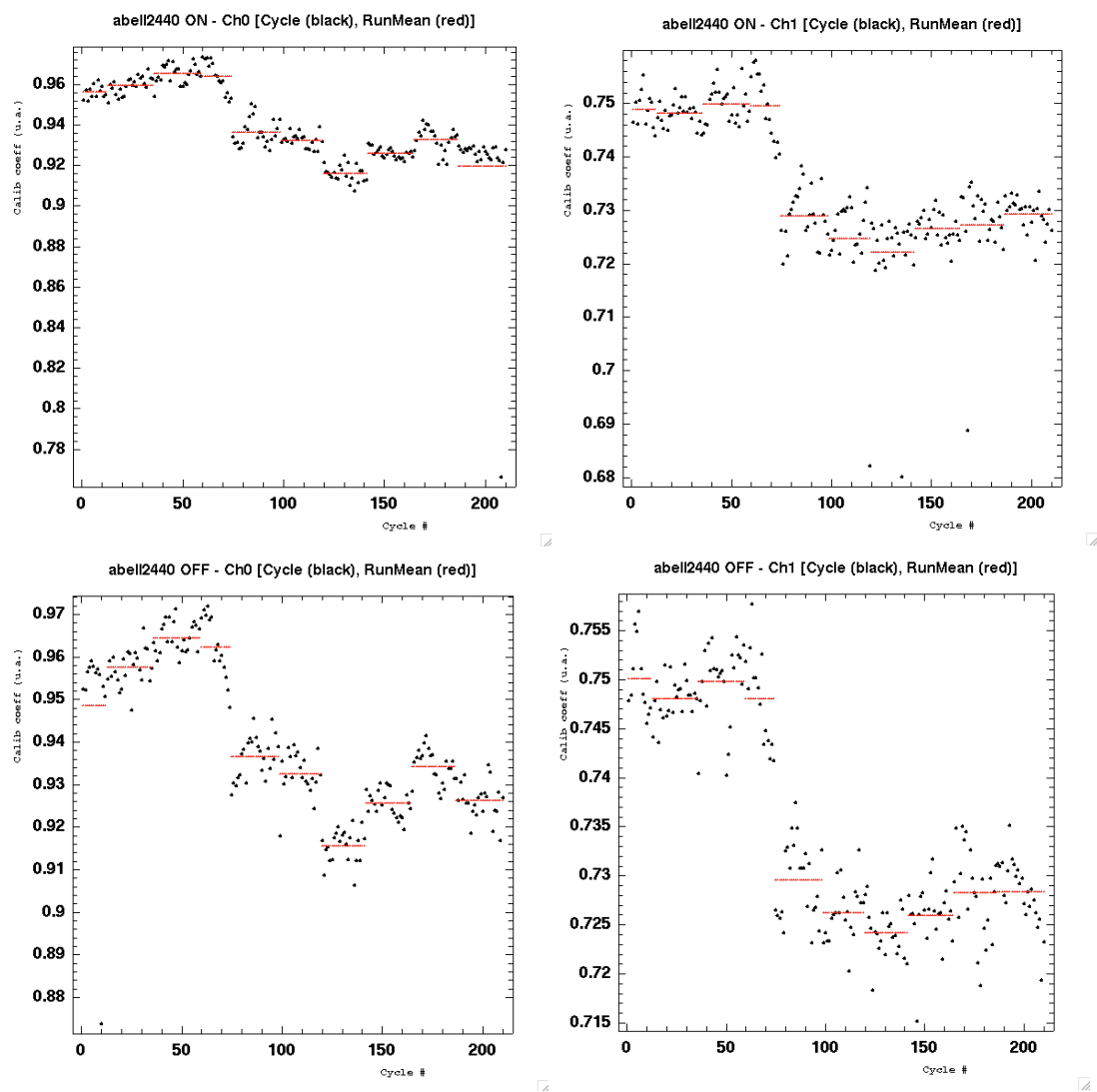


Figure 15. Calibration coefficients per cycle (black) and per run (red) vs. cycle number. Top : ON mode for channel 0 (left) and channel 1 (right). Bottom : idem for mode ON.

B.2 T_{sys} evolution vs. calibration coefficients

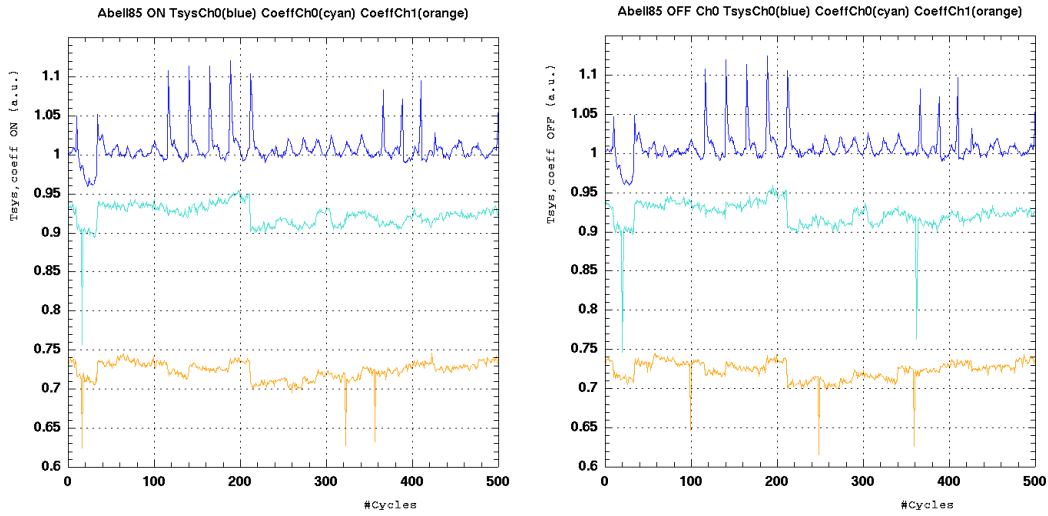


Figure 16. System noise (T_{sys} , blue) and calibration coefficients for Ch0 (cyan) and Ch1 (orange) vs. cycle number for OFF (left) and ON (right) modes.

B.3 Effect of calibration in signal data

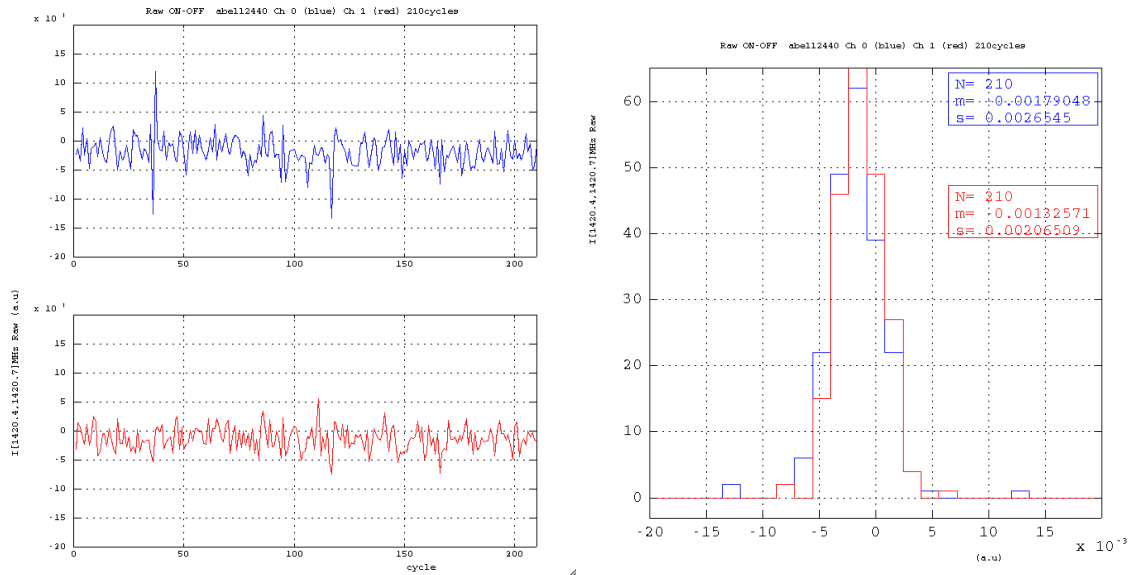


Figure 17. Integrated ON-OFF mean intensity from the galactic HI line without calibration. Signal evolution (left) and mean and sigma of the previous plot (right).

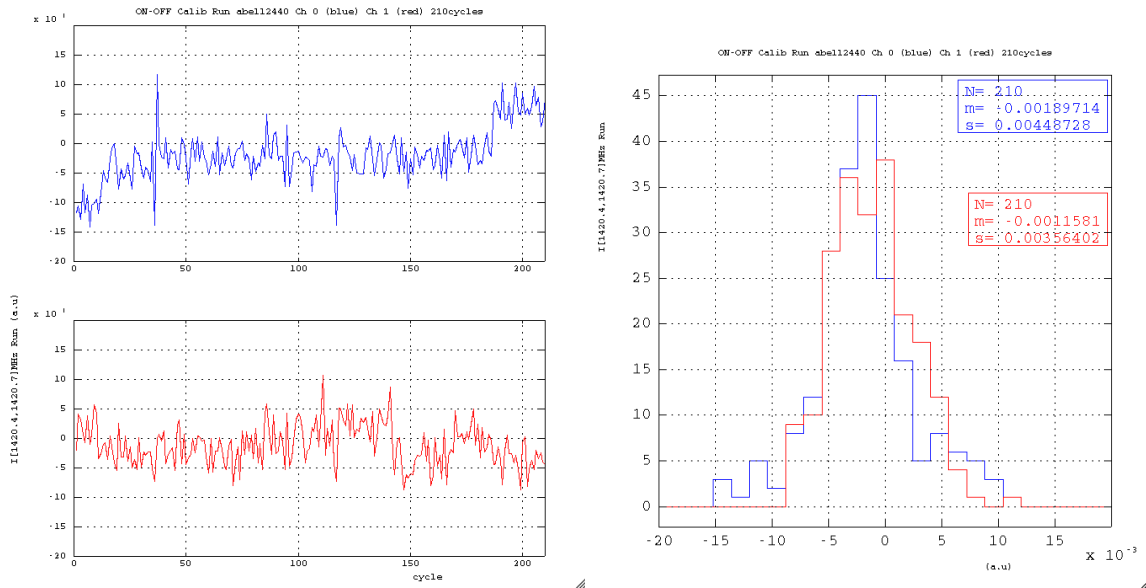


Figure 18. Integrated ON-OFF intensity from the galactic HI line calibrated with coefficients “per run”. Signal evolution (left) and mean and sigma of the previous plot (right).

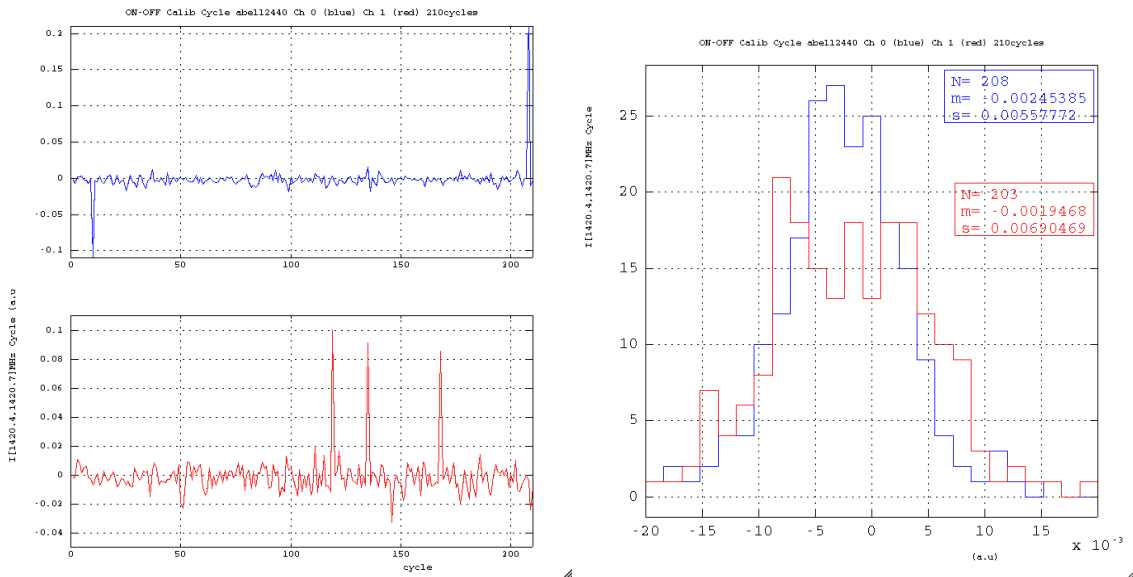


Figure 19. Integrated ON-OFF intensity from the galactic HI line calibrated with coefficients “per cycle”. Signal evolution (left) and mean and sigma of the previous plot (right).